Structural proteomics defines a sequential priming mechanism for the progesterone receptor

Matthew D. Mann[1,2], Min Wang[3], Josephine C. Ferreon[5], Michael P. Suess[3], Antrix Jain[4] Anna Malovannaya[5], Bruce D. Pascal[6], Raj Kumar[7], Dean P. Edwards[3], and Patrick R. Griffin[*,1,2]

[1]Skaggs Graduate School of Chemical and Biological Sciences, The Scripps Research Institute, Jupiter, FL, USA.

[2]Department of Molecular Medicine, The Herbert Wertheim UF Scripps Institute for Biomedical Innovation & Technology, Jupiter, FL, 33458

[3] Department of Molecular and Cellular Biology, Baylor College of Medicine, Houston, TX, 77030 USA.

[4] Mass Spectrometry Proteomics Core Facility. Advanced Technology Cores, Baylor College of Medicine, Houstonm TX, 77030

[5] Verna and Marrs McLean Department of Biochemistry and Molecular Pharmacology, Baylor College of Medicine, Houston, TX, 77030

[6] Omics Informatics LLC. 1050 Bishop Street #517, Honolulu, HI 96813

[7] Department of Pharmaceutical and Biomedical Sciences, Touro College of Pharmacy, Touro University, New York, NY, USA.

* Correspondence should be addressed to pgriffin2@ufl.edu

Running title: Structural proteomics reveals a unique activation model for PR-A and PR-B

Acknowledgements: This work was supported by NIH-NCI R01 (CA263574) to MPIs, PRG, RK, and DPE. The authors acknowledge the expert assistance of the Recombinant Protein Production and Characterization Core (RPPCC) for expression of recombinant proteins in the baculovirus insect cell system and the Mass Spectrometry Proteomcs (MSPC) Core for amino acid sequencing and phosphorylation analysis of recombinant proteins. The RPPCC and MSPC at BCM are supported by the NCI Cancer Center Support Grant (P30 CA125123) of the Dan L Duncan Comprehensive Cancer Center and the MSPC is additionally supported by a CPRIT (Cancer Prevention and Research Institute of Texas) Core Facility Support Award (RP210227). Additional support is from NIH S10 Shared Instrument Grant (1S10OD030276) to JCF for the SEC-MALS instruments.

Keywords:

Progesterone receptor; hydrogen-deuterium exchange; crosslinking; mass spectrometry; protein-protein interactions; nuclear receptors, transcriptional co-regulatory proteins

Supplemental Figures

1. **Affinity/SEC two-step purification of SII-tagged PR**
2. **Mass Spectrometry sequencing of purified major PR-A and PR-B bands**
3. **Mass Spectrometry sequencing of minor smaller molecular sized band product with PR-B**
4. **Affinity/SEC two-step purification for SRC3 tagged SII**
5. **Affinity/SEC two-step purification for p300 tagged SII**
6. **Mass Spectrometry of purified SRC3 and p300**
7. **SEC MALS of PR-A/SRC3/p300/DNA Complex**
8. **Differential scanning fluorimetry (DSF) analysis of PR-A with and without DNA**
9. **Intrinsic deuterium exchange for PR-A and PR-B**
10. **HDX overlays on best HDXer models of PR-B:SRC3 complexes**
11. **Workflow for PR:SRC3 model generation and selection**
12. **Deuterium exchange differences align with crosslinking results**
13. **Crosslinking shows NR-Box 3 is exclusively used by p300**
14. **Mutation of NR-box 2 or dual combination mutants to LXXAA in SRC3 reduces PR activity**
15. **SEC-MALS of purified PR-A and PR-B bound to the progestin antagonist RU486 with and without DNA**

Supplemental Tables

1. **SEC-MALS Experimental vs Theoretical MWs of individual purified proteins and various mixtures in the presence and absence of DNA**
2. **Transition melting temperatures (T_M) of each purified protein as determined by DSF**

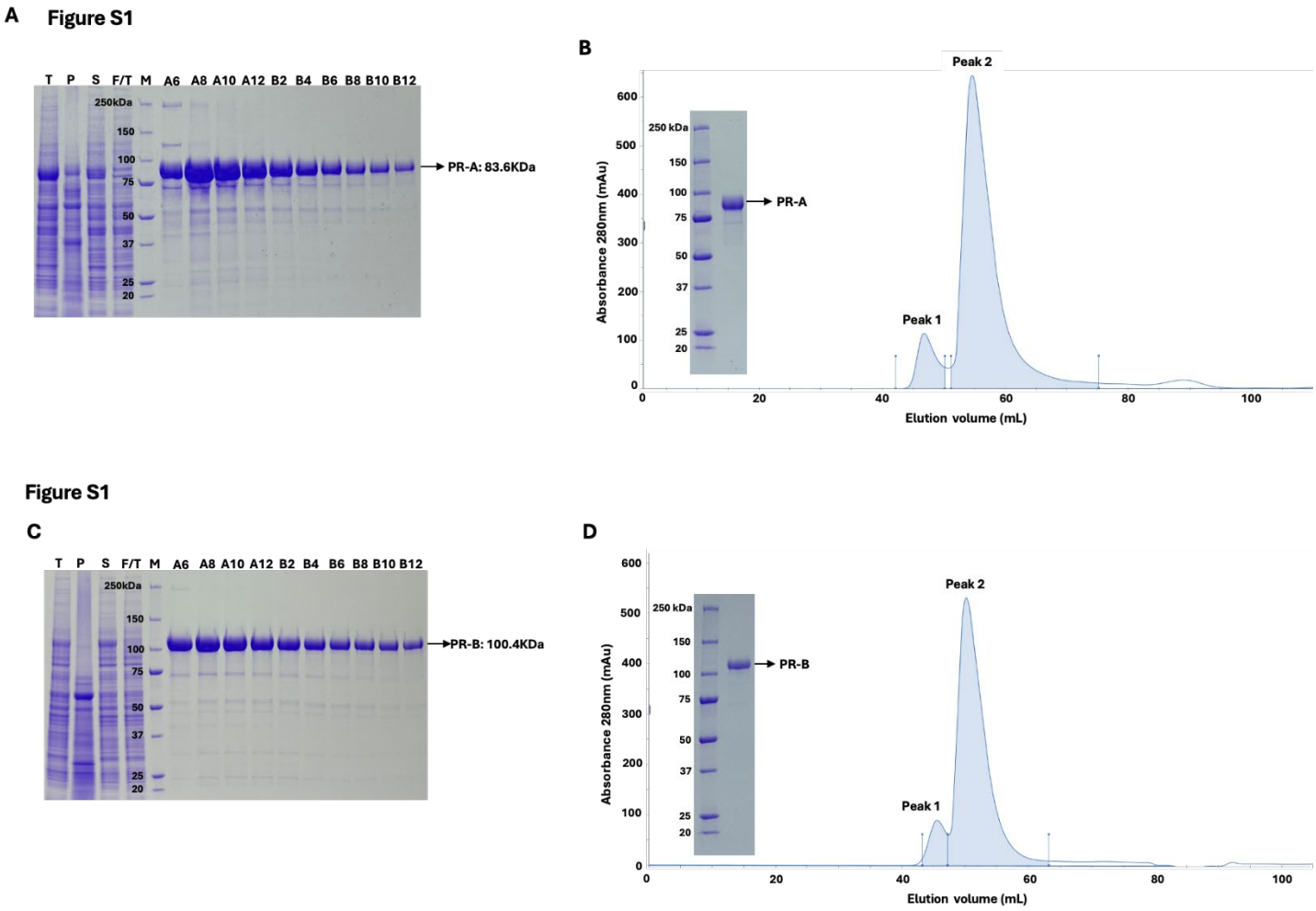

Fig S1. Affinity/SEC two-step purification of SII-tagged PR. SII-tagged PR-A and PR-B were expressed in Sf9 cells and cell lysates were prepared and purification performed by two -step affinity Strep Trap XT column and size exclusion chromatography (SEC) S200 as described in Methods. *A)* SDS-PAGE analysis of PR-A affinity purification fractions T, total cell lysate, P pellet after centrifugation lysate, S supernatant after centrifugation, F/T flow through after binding to Strep TrapXT, M, protein molecular weight markers. Lanes A6-B12 (5uL) biotin eluted fractions with major enriched protein bands at expected size of ~83 kDa for PR-A. *B)* SEC fractionation of pooled fractions A6-B12 off the Strep Trap XT column. OD tracing at 280nM shows major peak 2 of monomeric size for PR-A and peak 1 containing high molecular weight aggregation. Peak 2 fractions were pooled, concentrated and analyzed SDS-PAGE gel showing a single band of >98% purity of the expected size of PR-A. C) *A)* SDS-PAGE analysis of PR-B affinity purification fractions and D) SEC second step purification by the same set-up and as PR-A except major band and purified product are expected size for monomeric PR-B (~100kDa).

Fig S2. Mass Spectrometry sequencing of purified major PR-A and PR-B bands.

Fig S3. Mass Spectrometry sequencing of minor smaller molecular sized band product with PR-B

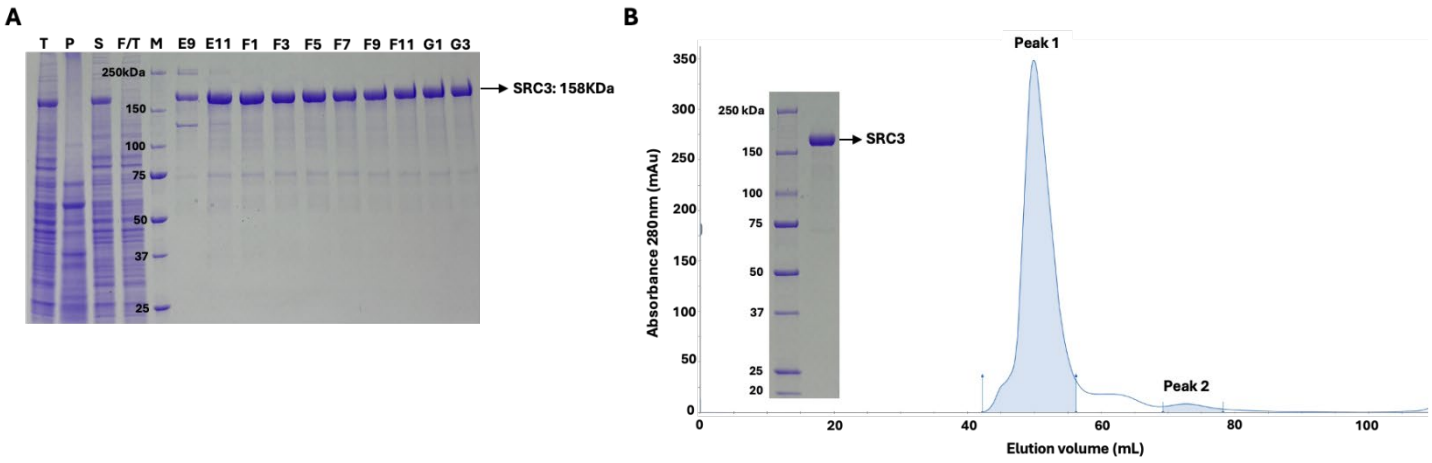

Fig S4. Affinity/SEC two-step purification for SRC3 tagged SII. SII-tagged SRC3 was expressed in Sf9 insect cells and purification performed by two -step affinity by StrepTrap XT and size exclusion chromatography (SEC) S200 as described in Methods. *A)* SDS-PAGE analysis of affinity purification fractions T, total cell lysate, P pellet after centrifugation, S supernatant after centrifugation, F/T flow through after binding to Strep TrapXT M, protein molecular weight markers. Lanes E9-H7 are SDS-PAGE analysis (5uL) of biotin eluted fractions with a major enriched band of expected size of ~158kDa for SRC3. *B)* SEC of pooled fractions E9-H7. OD tracing at 280nM shows a major peak (peak 1) of the native size expected for SRC3 and a minor peak (peak 2) of lower molecular weight protein. Peak 1 fractions were pooled, concentrated and analyzed by SDS-PAGE showing a single band of >98% purity of the expected size of SRC3.

.

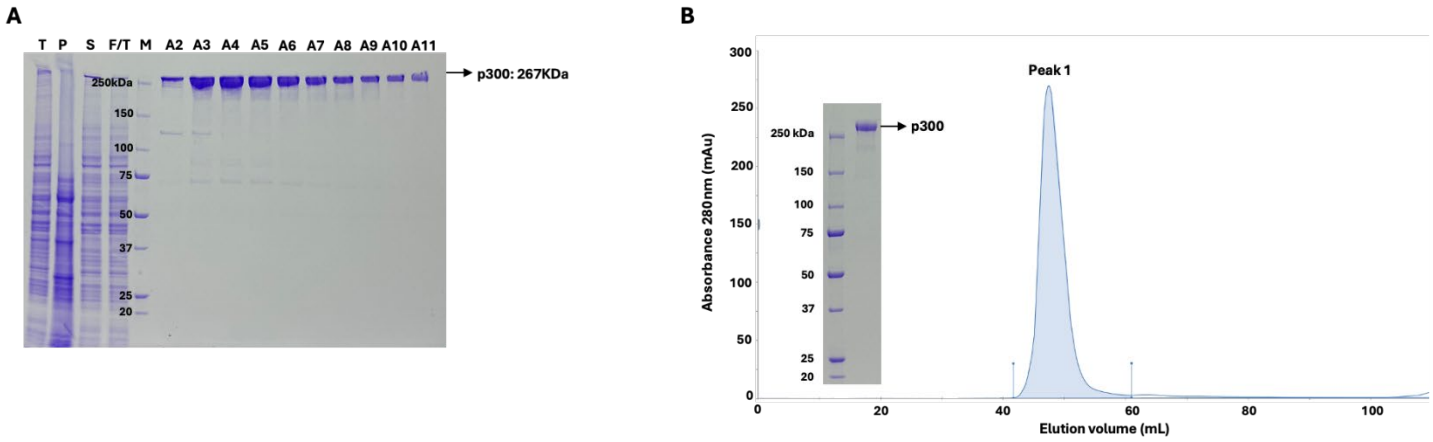

FigS5 Affinity/SEC two-step purification for p300 tagged SII. SII-tagged p300 was expressed in Sf9 insect cells and purification performed by two -step affinity by StrepTrap XT and size exclusion chromatography (SEC) S200 as described in Methods. *A)* SDS-PAGE analysis of affinity purification fractions T, total cell lysate, P pellet after centrifugation, S supernatant after centrifugation, F/T flow through after binding to Strep TrapXT M, protein molecular weight markers. Lanes A2-A11 are SDS-PAGE (5uL) of biotin eluted fractions with a major enriched bands of the expected size for p300 (~267kDa). *B)* SEC of pooled fractions from Strep TrapXT shows a single major peak (OD tracing at 280nM). The pooled SEC fractions on SDS-PAGE analysis show a single major band of the expected sized for p300.

Fig S6. Mass Spectrometry of purified SRC3 and p300.

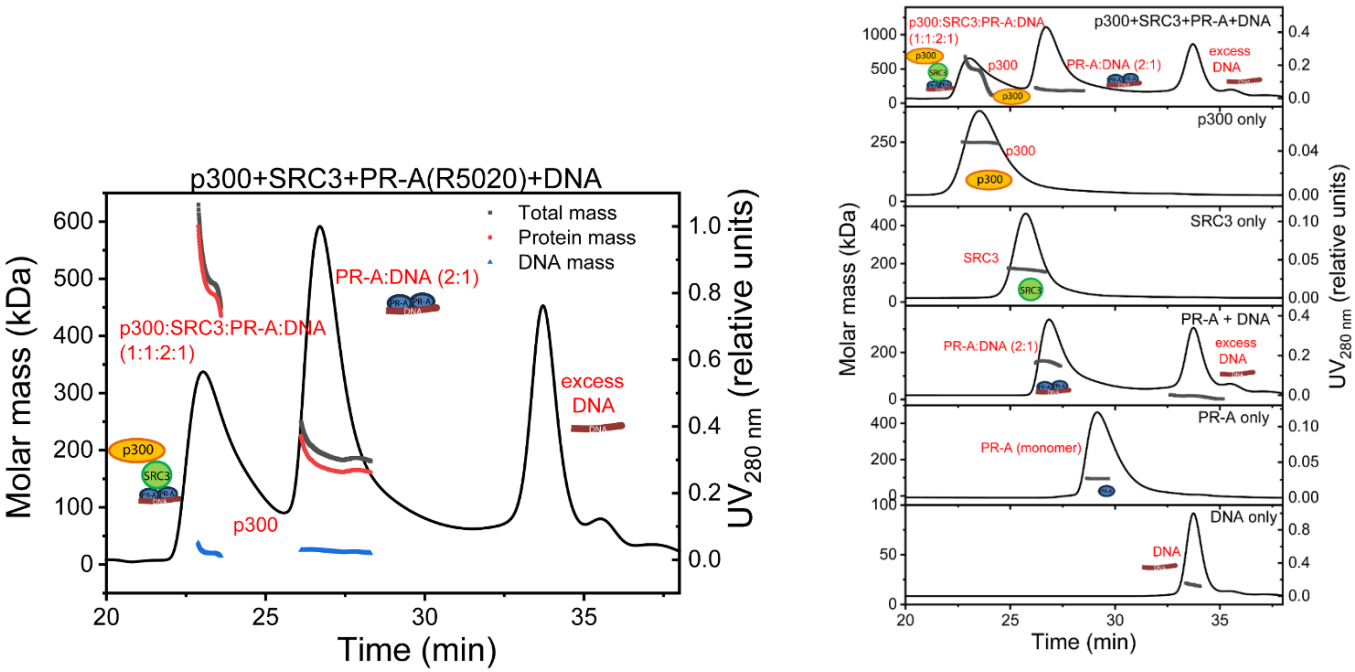

Fig S7 SEC MALS of PR-A/SRC3/p300/DNA Complex. SEC-MALS chromatograms with molar mass distribution for various proteins, DNA and in complexes. PR-A (with agonist R5020) assembles only to a dimer in the presence of DNA. A multi-complex of p300:SRC3:PR-A:DNA at a 1:1:2:1 ratio is observed (top chromatogram). The presence of DNA is also confirmed by deconvolution of the protein and DNA fractions in the peak. Assembly of multi-protein p300:SRC3:PR-A with DNA. SEC-MALS chromatogram of p300:SRC3:PR-A: DNA complex. The fractional contributions of the proteins and DNA mass are displayed as red and blue symbols, respectively. The full complex showed a heterogeneous distribution of molar mass due to overlap with the p300 monomeric peak.

Table S1. SEC-MALS Experimental vs Theoretical MWs of individual purified proteins and various mixtures in the presence and absence of DNA.

Table 1. SEC-MALS derived molecular weights for proteins, DNA and the complexes formed

	Theoretical MW	Actual MW[a]	
Protein/DNA		**by UV**	**by dRI**
DNA	19.6	18.2 ± 0.9	20.1 ± 1.0
PR-A(R5020)	83.6	94.9 ± 4.8	91.2 ± 4.6
PR-A(RU486)	83.6	98.8 ± 4.7	95.3 ± 4.8
PR-B(R5020)	100.4	116.4± 5.8	101.6± 5.1
PR-B(RU486)	100.4	96.3 ± 4.8	97.7 ± 4.10
p300	267	249.2 ± 12.5	200.5 ± 9.2
SRC3	158	170.3 ± 8.5	159.7 ± 8

Complexes	**Theoretical MW**	**Actual MW**
PR-A(R5020):DNA (2:1)	186.8	161.6 ± 8.1
Protein component	167.2	144.8 ± 7.2
DNA component	19.6	16.8 ± 0.8
PR-A(RU486):DNA (2:1)	186.8	189.3 ± 9.5
Protein component	167.2	167.5 ± 8.4
DNA component	19.6	21.8 ± 1.1
PR-B(R5020):DNA (2:1)	220.4	224.0 ± 11.2
Protein component	200.8	201.7± 10.1
DNA component	19.6	22.3 ± 1.1
PR-B(RU486):DNA (2:1)	220.4	221.8 ± 11.1
Protein component	200.8	197.7± 9.9
DNA component	19.6	24.1 ± 1.2
p300:SRC3:PR-A(R5020):DNA (1:1:2:1)	611.8	536.5 ± 26.8[b]
Protein component	592.2	512.7 ± 25.6
DNA component	19.6	23.7 ± 1.2
PR-A(R5020):DNA (2:1)[c]	186.8	190.7 ± 9.5
Protein component	167.2	161.4 ± 8.1
DNA component	19.6	29.3 ± 1.5

[a] errors are 5% of calculated MW; dn/dc based off BSA values in similar buffer condition

[b] heterogeneous MW distribution, overlap with p300

[c] in same buffer conditions as above but with 0M Urea

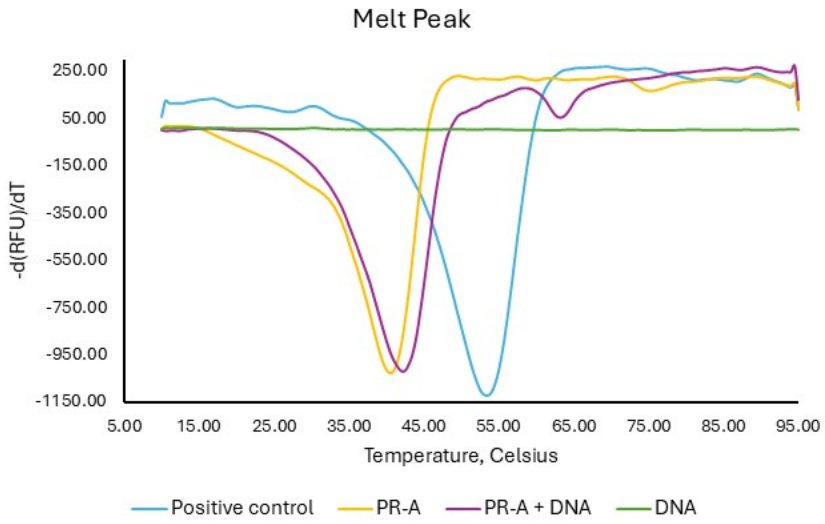

Fig S8. Differential scanning fluorimetry (DSF) analysis of PR-A with and without DNA. DSF analysis of 4ug TLX-WT (as the positive control, blue), PR-A (yellow) and PR-A plus PRE DNA (purple).

Table S2. Transition melting temperatures (T_M) of each purified protein as determined by DSF.

Protein	T_m (°C)
PR-A	40.7±0.3
PR-A + DNA	42.2±0.3
PR-B	43.5±0
PR-B + DNA	45.0±0
p300	49.1±0
SRC3	46.5±0.1

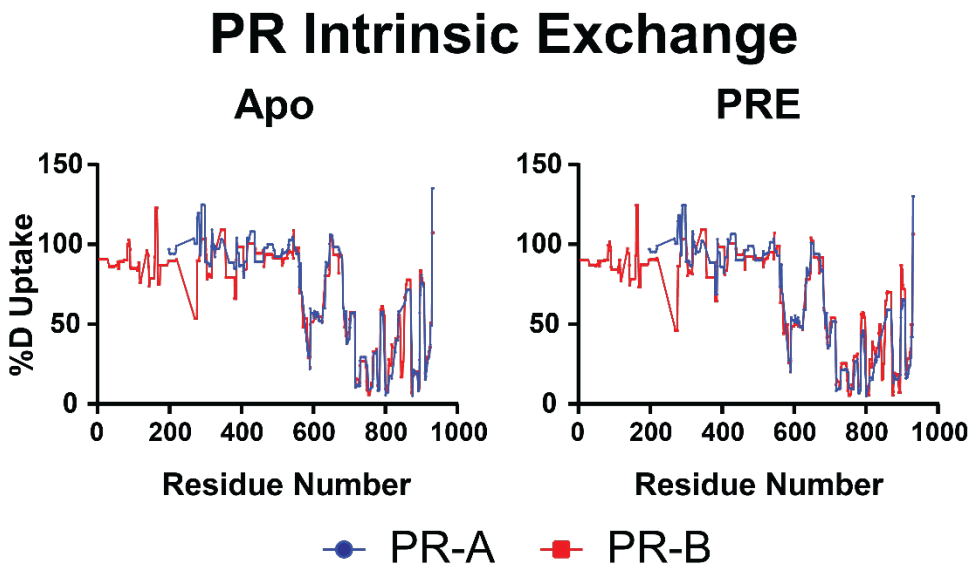

Figure S9. **Intrinsic deuterium exchange for PR-A and PR-B**. Woods plots showing the percent deuterium exchange (%D Uptake) for both PR-A (blue) and PR-B (red) across each residue across the protein in both non-DNA-bound (Apo) and DNA-bound (PRE) states. Graphs made using GraphPad Prism 10.

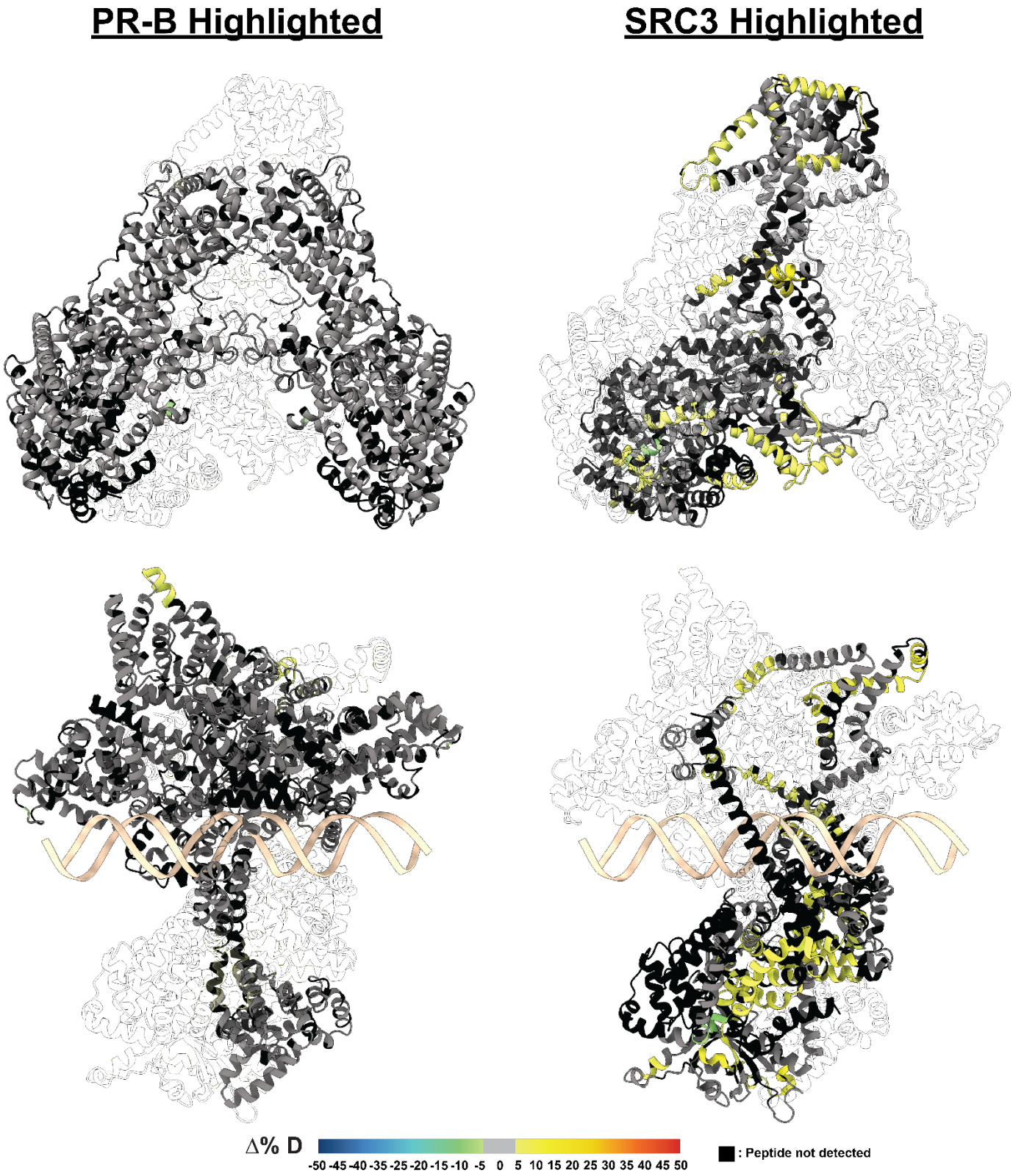

Figure S10. HDX overlays on best HDXer models of PR-B:SRC3 complexes. HDX-MS overlays on best selected model of PR-B:SRC3 complex in both non-DNA-bound (top) and DNA-bound (bottom) states. Warmer colors (yellow, orange, red), indicate increased deuterium exchange, and cooler colors (green, blue) indicate decreased deuterium exchange. Black indicates the peptide was not found by HDX and gray indicates exchange within ±5%. Models selected by HDXer RMSE values, and visualizations made using ChimeraX 1.8.

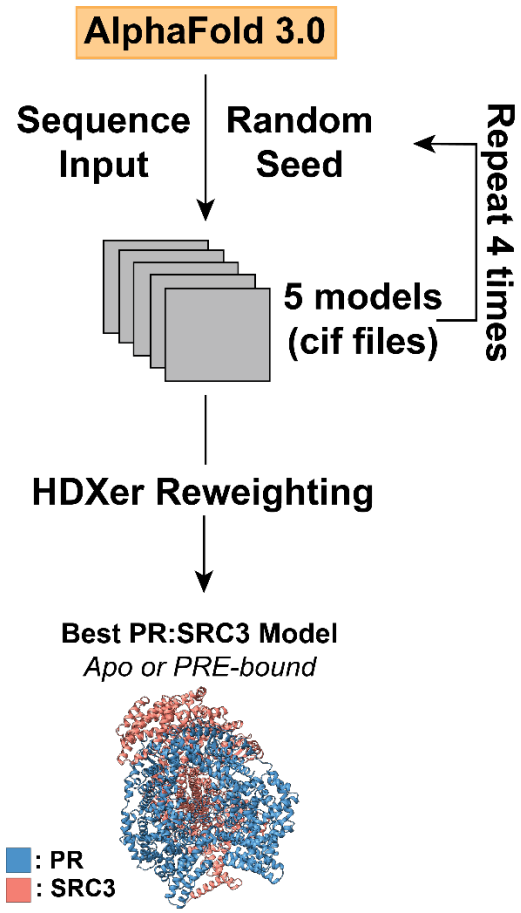

Figure S11 Workflow for PR:SRC3 model generation and selection. Workflow detailing the model generation for ternary complexes. AlphaFold3.0 webserver was used to generate PR:SRC3 models in quintuplicate. Models were ensemble reweighted using HDXer (see methods) to determine best representation based on HDX data.

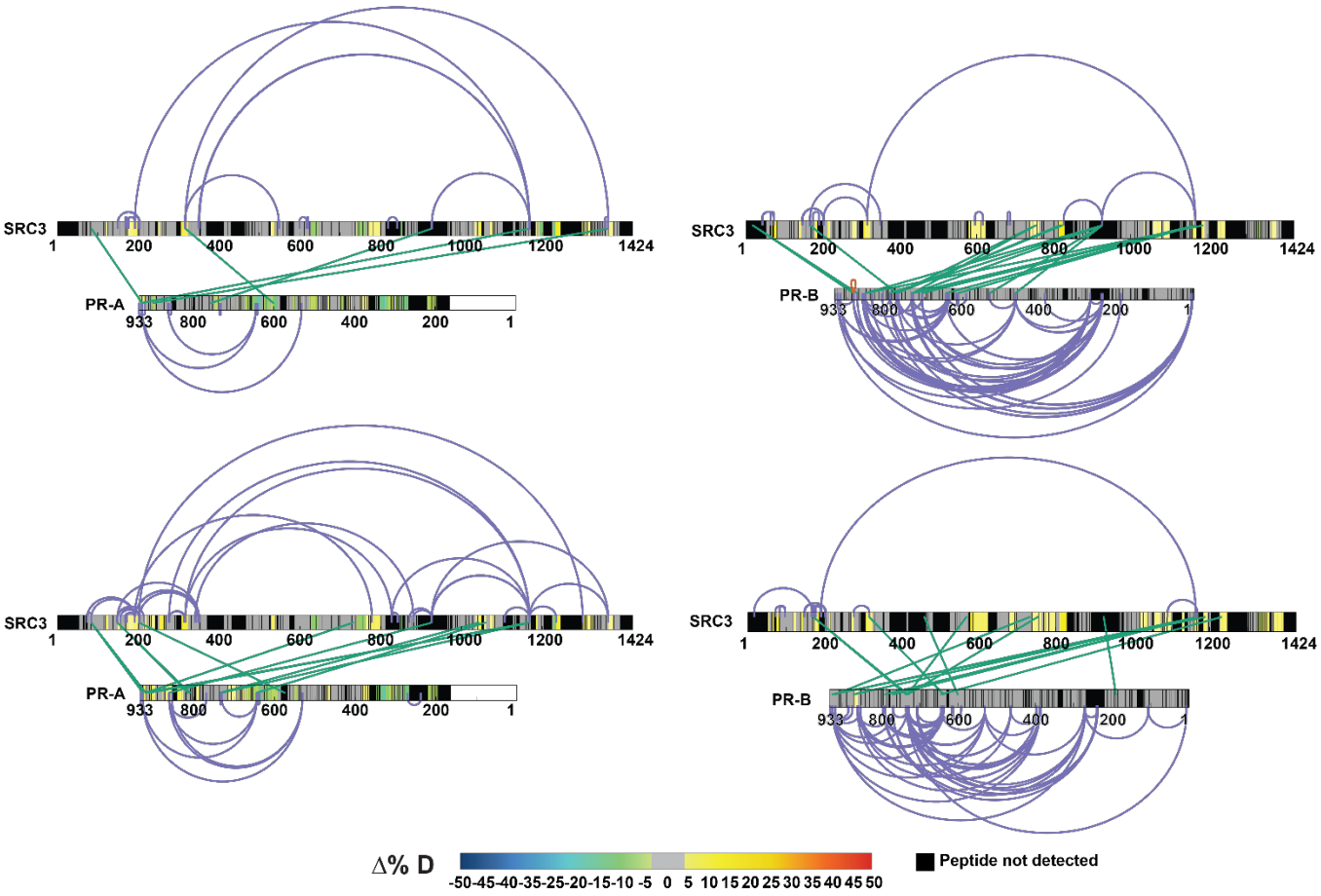

Figure S12. PR and SRC3 deuterium exchange differences align with crosslinking results. A. XiView images of differential XL-MS data for PR-A vs. PR-A:SRC3 experiments with crosslinks enriched in apo samples (top) and pre-bound samples (bottom) represented. HDX overlays are indicative of their comparable differential HDX-MS experiments. Top: SRC3 exchange - SRC3 vs. PR-A:SRC3 (non-DNA bound), PR exchange – PR-A vs. PR-A:SRC3. Bottom: SRC3 exchange – SRC3 vs. PR-A:SRC3:PRE, PR exchange – PR-A:SRC3 vs. PR-A:SRC3:PRE. **B.** XiView images of differential XL-MS data for PR-B vs. PR-B:SRC3 experiments with the same HDX overlays as shown in **A.** Intraprotein crosslinks are represented in purple, interprotein crosslinks are represented as green. Differential HDX-MS scale shows the % change in deuterium incorporation, where cooler colors represent reduced deuterium exchange, while warmer colors (yellow, orange, red) represent increased deuterium exchange. Black represents peptides not detected in HDX-MS experiments, and PR isoforms have numbering normalized to the B isoform.

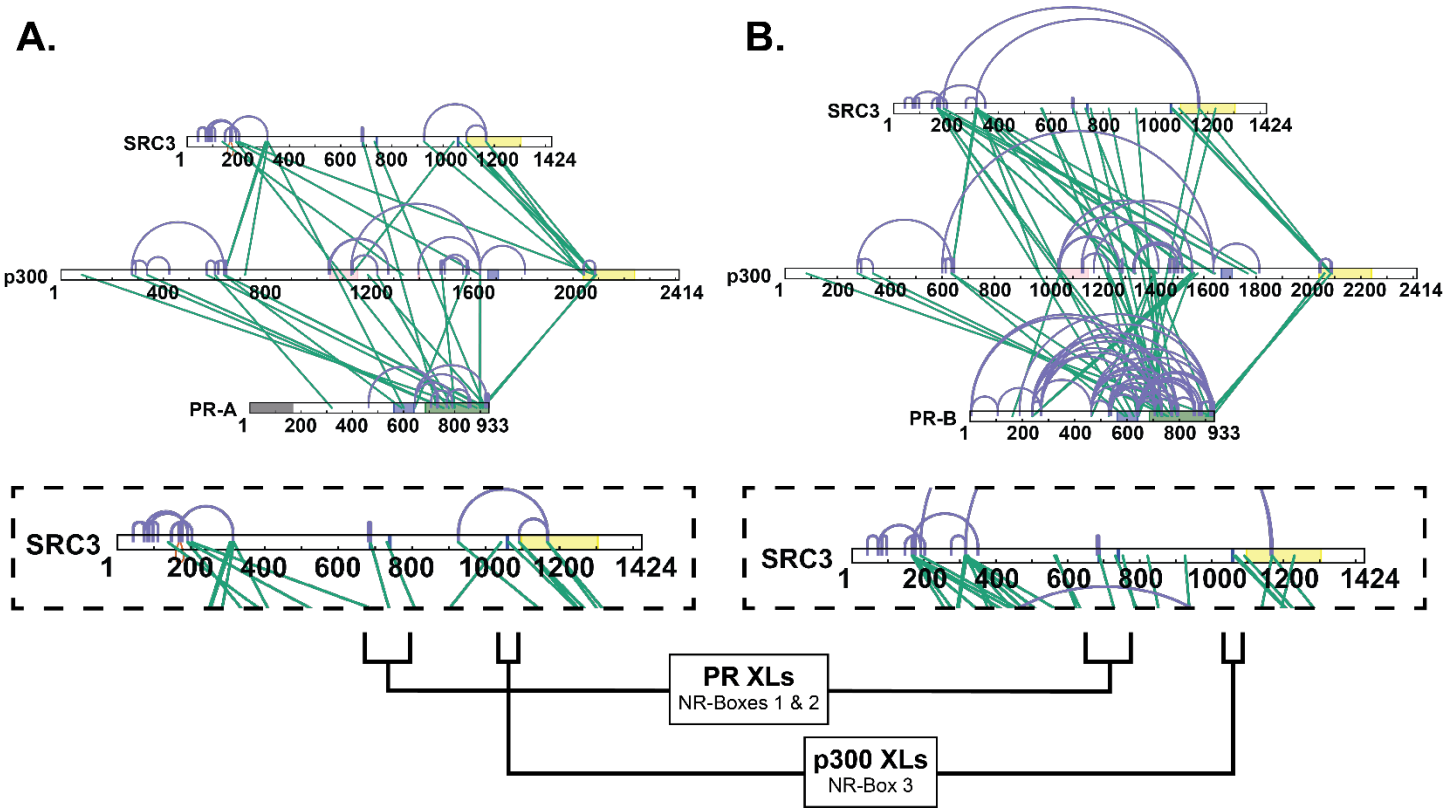

Figure S13. Crosslinking shows NR-Box 3 is exclusively used by p300. A. Top: All validated crosslinks from differential PR-A:SRC3:p300±PRE experiments. Bottom: Zoomed in view of SRC3 to show NR-Box crosslinks specific to the PR-A-containing complex. **B.** Top: All validated crosslinks from differential PR-B:SRC3:p300±PRE experiments. Bottom: Zoomed in view of SRC3 to show NR-Box crosslinks specific to the PR-B-containing complex. Defined domains are as follows: PR - DBD (purple) and LBD (green); SRC3 – NR-boxes (purple) and histone acetyltransferase domain (yellow); p300 - bromodomain (pink), zinc finger domain (green), and NCOA2-interaction domain (yellow).

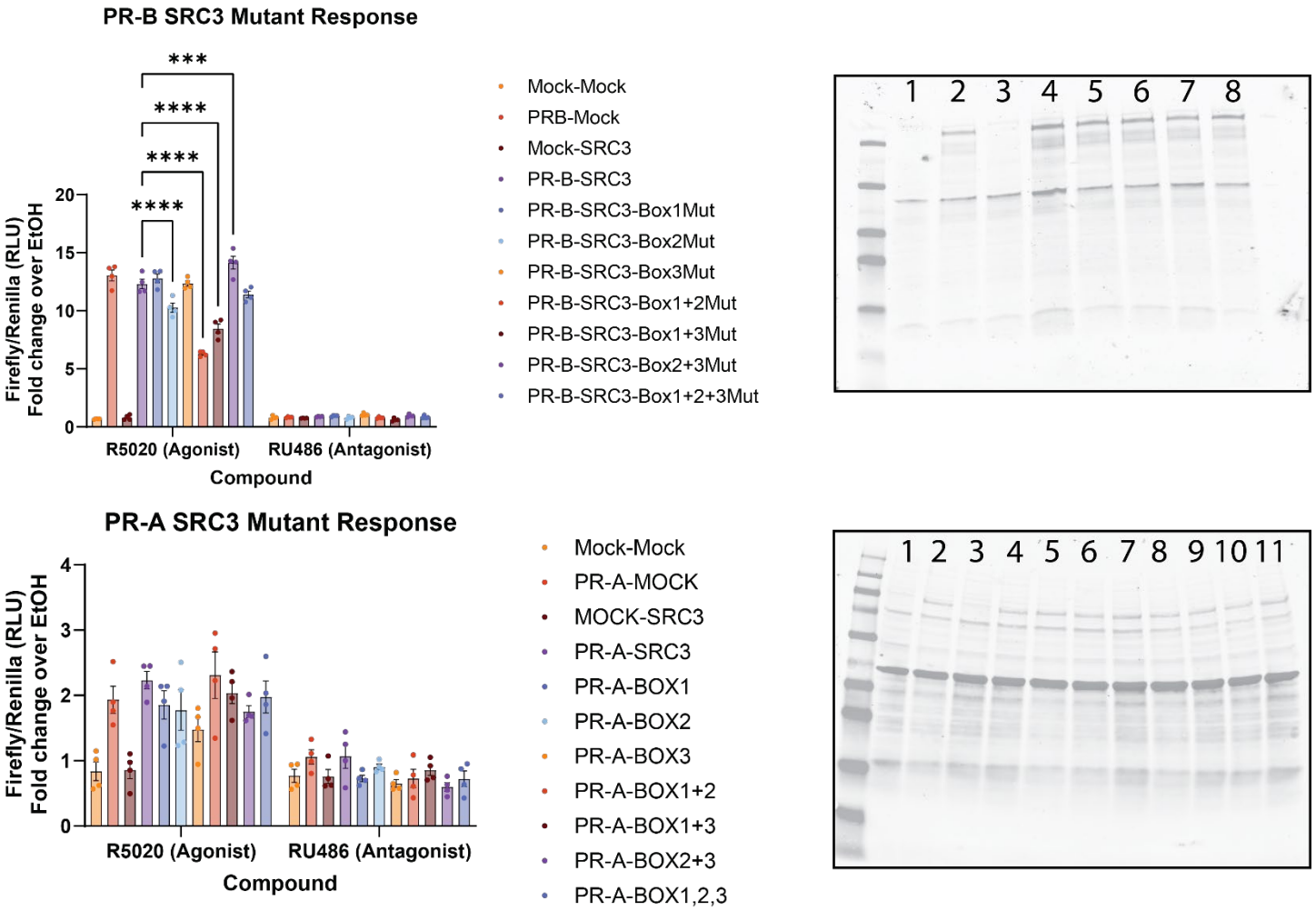

Figure S14. Mutation of NR-box 2 or dual combination mutants to LXXAA in SRC3 reduces PR activity. Bar graph showing the ratio of Firefly to Renilla luciferase normalized over the vehicle (ethanol) signal for both R5020 PR agonist and RU486 PR antagonist. Mock is indicative of water in the place of PR or SRC3 plasmid. 'Mut' in the legend indicates an LXXLL NR-Box mutated to LXXAA, validated by whole plasmid next-generation sequencing (Azenta). Points indicative of 4 replicates with SEM error bars. Two-way ANOVA was performed with Tukey correction for multiple comparisons, and asterisks indicate $p<0.001$ (***) and $p<0.0001$ (****).

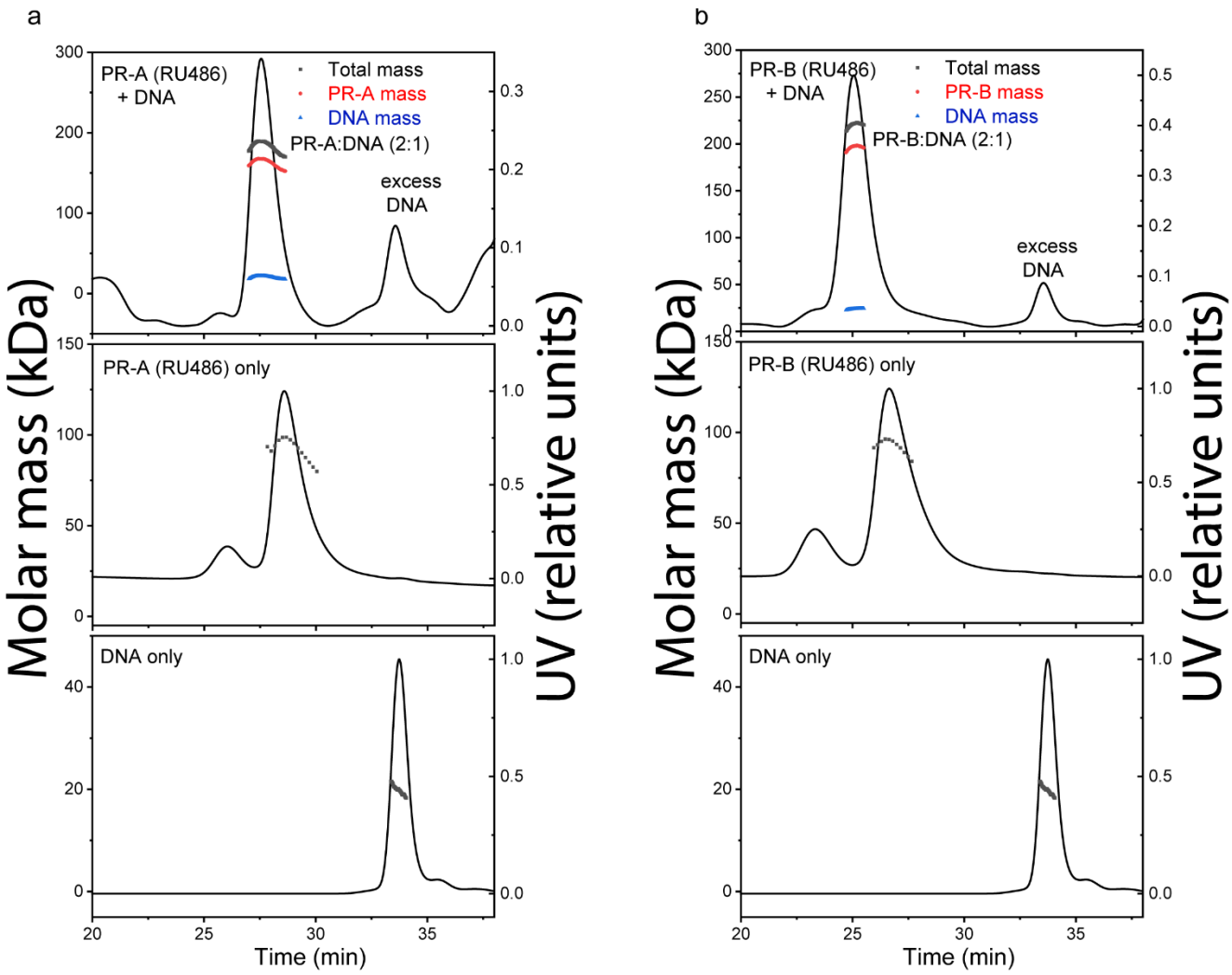

Fig S15. SEC-MALS of purified PR-A and PR-B bound to the progestin antagonist RU486 with and without DNA. DNA induces assembly of PR dimers A-B. SEC-MALS chromatograms of antagonist (RU486)- bound PR-A (A) and PR-B (B) with and without DNA. The molar mass of DNA and PR-A alone matches the monomeric molar mass (black line/dots across the peaks). DNA induces assembly of both PR-A and PR-B into a complex with 2:1 (protein:DNA) stoichiometry. The presence of DNA in the complexes were confirmed by deconvolution of the protein and DNA fractions in the peak (red and blue lines, respectively).